

FBMC Testbed with Frequency Domain Synchronization and Adaptive Bandwidth

Maxim Penner, Muhammad Nabeel, and Jürgen Peissig
Institute of Communications Technology, Leibniz Universität Hannover, Germany
{penner,nabeel,peissig}@ikt.uni-hannover.de

Abstract—To meet the ever growing demand of data rates, many modern wireless systems have adopted multicarrier modulation schemes. Nowadays, Orthogonal Frequency-Division Multiplexing (OFDM) is the most commonly used multicarrier modulation scheme that offers efficient use of bandwidth. To tackle intersymbol interference and avoid complex channel equalization, OFDM is usually used in combination with a Cyclic Prefix (CP). However, CP-OFDM comes with its own limitations such as the need of precise time and frequency synchronization, high out-of-band radiation as well high peak-to-average power ratio. Therefore, researchers have started investigating alternative multicarrier modulation schemes. Among others, Filter Bank Multicarrier (FBMC) is gaining a lot of attention due to its optimized prototype filters that eliminate the need of CP and reduce out-of-band radiation and, hence, offers further improvement in bandwidth utilization. In this work, we develop a Software Defined Radio (SDR) based FBMC testbed that operates in real time. We use GNU Radio as a software part of SDR in combination with Universal Software Radio Peripherals (USRPs) for over-the-air experiments. In contrast to state of the art, our FBMC transceiver exploits frequency domain synchronization and can easily be tuned for various bandwidths. By conducting over-the-air measurements, we show that the developed testbed can successfully be used even in presence of other narrowband systems in the same frequency bands. For the purpose of reproducibility, we make the testbed implementation also publicly available.

I. INTRODUCTION

Modern wireless systems have to transport ever growing amounts of data, but at the same time the available bandwidth is limited, especially in bands below 6 GHz. For this reason, many modern systems such as Long Term Evolution (LTE), New Radio (NR), and Wireless Local Area Network (WLAN) must utilize the given bandwidth more efficiently. This is achieved, amongst other measures, by increasing the number of transmit/receive antennas, exploiting flexible numerology, a highly variable resource unit assignment, higher modulation orders, or combinations of these techniques. Apart from these approaches, one option to achieve higher data rate is to use multicarrier modulation schemes. All of the aforementioned technologies use Orthogonal Frequency-Division Multiplexing (OFDM) in combination with Cyclic Prefix (CP). CP-OFDM offers many advantages in terms of bandwidth efficiency, channel estimation simplicity and overall system performance, however, it also has certain drawbacks such as the need of fine time and frequency synchronization and high out-of-band radiation. Therefore, in this work, we focus on Filter Bank Multicarrier (FBMC) as an alternative.

FBMC is a modern multicarrier scheme in which each subcarrier is filtered with an adjustable prototype filter, instead of a rectangular filter as is the case with CP-OFDM. This results in FBMC not requiring a CP, since intersymbol interference due to multipath propagation is mitigated by using optimized prototype filters. Compared to CP-OFDM, FBMC also has smaller side lobes and, hence, better selectivity. Thus, FBMC allows further improvements in bandwidth utilization and, as a result, the system becomes more flexible, allows guardbands between neighboring systems to be smaller due to the improved selectivity, and has less out-of-band radiation. This new flexibility even extends to the point where wireless systems can be interleaved: A wideband FBMC system could, by leaving a set of subcarriers empty, create deep notches within its own bandwidth, in which a second (non-FBMC) system can coexist independently and with minimal interference. Theoretically, such a system can also be built with CP-OFDM, however, considerably more subcarriers would have to be left empty for the same depth of notch due to large side-lobes.

FBMC is a theoretically well-studied modulation scheme, but there are only a few testbeds available [1], [2]. In [1], authors present an FBMC testbed in combination with Multiple Input Multiple Output (MIMO). The testbed is Software Defined Radio (SDR) based, uses LTE frame structures, and achieves a bandwidth of 8 MHz. The main focus is to measure the suitability of FBMC for MIMO at the physical layer, accordingly the target metrics are bit error rate and peak-to-average power ratio. It is concluded that FBMC and MIMO are compatible and the performance is comparable to that of OFDM. While this involves more algorithmic complexity, it is nonetheless a positive result, as it is often assumed that FBMC and MIMO are mutually incompatible. In [2], another FBMC testbed is presented that is also SDR-based. The authors use the testbed for a situational awareness scenario, in which they try to learn the transmission pattern of a primary user, so that a secondary user can maximize its own throughput without interfering with the primary user. The signal of the secondary user utilizes FBMC because of its low out-of-band radiation. Synchronization is performed in the time domain and the focus of the work primarily lies on detecting the primary user by using energy and preamble detection.

In this work, we develop a real time FBMC testbed. It consists of a broadband FBMC transceiver that autonomously detects a coexisting system in real time and continuously adjusts its own bandwidth used for data transmission so that

both systems can transmit simultaneously. In order to use such interleaved systems, we also introduce a novel feature by utilizing synchronization in frequency domain. This is in contrast to available FBMC testbeds and other OFDM systems such as WLAN that perform preamble synchronization in time domain across the full system bandwidth. In our case, the unsynchronized signal is first transformed into frequency domain, where parts of the spectrum can then be selectively excluded prior to synchronization. The part of the spectrum used by the coexisting system is ignored to enable an optimal synchronization process. To the best of our knowledge, there is no FBMC testbed in literature that combines real time capabilities with frequency synchronization and bandwidth adaption. Our system is developed in GNU Radio, a popular framework for the development of wireless systems, and can be operated with commercially available SDR devices. We also publish the whole project in an open-source repository to ensure verifiability for other researchers and to allow further development and testing.

Our main contributions can be summarized as follows:

- We develop an SDR-based FBMC testbed and provide details of both transmitter and receiver chains of the transceiver. We explain the process of bandwidth adaption at the transmitter and frequency synchronization at the receiver (Section II).
- We demonstrate our testbed capabilities and conduct various measurements with a spectrum analyzer (Section III).
- We make our source code publicly available on Github.¹

II. SYSTEM MODEL

In this section, we discuss the developed transceiver and its operation in detail. Both the transmitter and the receiver chain can be operated independently and are explained below.

A. Transmitter

As mentioned earlier, we use GNU Radio in combination with SDR devices. The latter are used for signal upconversion/downconversion and transmitting/receiving IQ samples, while the baseband processing is performed in software using GNU Radio on personal computers. The achievable signal bandwidth is primarily dependent on the processing power of the computer, which in our case is 12.5 MHz nominal bandwidth. In our indoor lab environment, we utilize 64 subcarriers of which a total of up to 52 can be occupied, four of them as pilot tones as shown at the top of Figure 1. On the right side of the spectrum, a gap (red diagonal stripes in Figure 1) can be created by zeroing subcarriers. Thus, there are a total of five possible subcarrier allocations: the full bandwidth or one of the fourth allocations shown with a gap. All possible allocations must be known a priori to all FBMC transceivers.

The transmitter generates FBMC data packets consisting of a preamble and a data part, similar to WLAN. The preamble is used for synchronization and consists of two equal FBMC symbols, similar to that in [3]. The maximum length of the

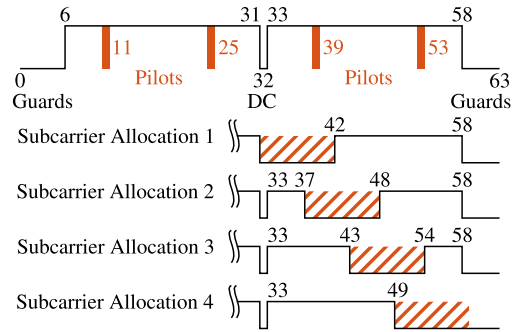


Figure 1: The FBMC transmitter can use different allocations of the 64 subcarriers (index 0, 1, . . . 63). It can either use the full bandwidth as shown at the top, or deactivate subcarriers and by that create a gap (red diagonal stripes) on the right side of the spectrum.

data part can be chosen depending on the application, but never exceeds 1472 B, the maximum transmission unit of Ethernet. It is noted that if a subcarrier allocation with a gap is used, the respective subcarriers are neither used for the preamble nor for the data part.

The structure of the transmitter is shown in Figure 2. Binary data is first received in the *UDP Data* block. Then the data is segmented and simultaneously a subcarrier allocation is selected according to Figure 1. In the block *MAC & PHY Encoder*, the segmented data packets are prefixed with a MAC and a PHY header, the latter containing data about the packet length and the selected modulation level etc. In addition, the data is channel coded with a convolutional code. In the *Carrier Allocator*, the subcarriers of each symbol are then filled with the complex Quadrature Amplitude Modulation (QAM) values of the preamble, pilot tones, and data.

In the subsequent block *OQAM*, which stands for Offset QAM (OQAM), the complex symbols are split into real and imaginary part, resulting in real symbols of twice the amount. If we denote the symbol index after this doubling by m and the real values of each symbol by $d_{k,m}$, the output signal of the transmitter is given by [4]

$$s[nT_s] = \sum_m \sum_{k \in K_u} j^{m+k} d_{k,m} p[nT_s - mT/2] e^{j \frac{2\pi}{T} knT_s}, \quad (1)$$

with the sampling rate $1/T_s$, the subcarrier index k , the set of occupied subcarriers K_u , and the real-valued prototype filter $p[\cdot]$. Besides splitting the symbols, the block *OQAM* also performs the multiplication with the factor j^{m+k} , and the prototype filter $p[\cdot]$ is applied in the block *PPN*, which stands for Polyphase Network (PPN). Finally, the signal is passed to the SDR device, in our case a Universal Software Radio Peripheral (USRP), and transmitted via the antenna.

In order to be adaptive to coexisting wireless systems, the transmitter needs to know if any portion of the spectrum is already occupied. For this, the USRP switches at least every 100 ms to receive mode for a short period of time and feeds samples into the blocks of the spectrum monitoring, i.e., *FFT* and *Channel Measurement*. A test is performed to determine if the power in any subcarriers exceeds a predefined threshold. If this is the case, it is assumed that another

¹www.github.com/maxpennner/gr-fbmc

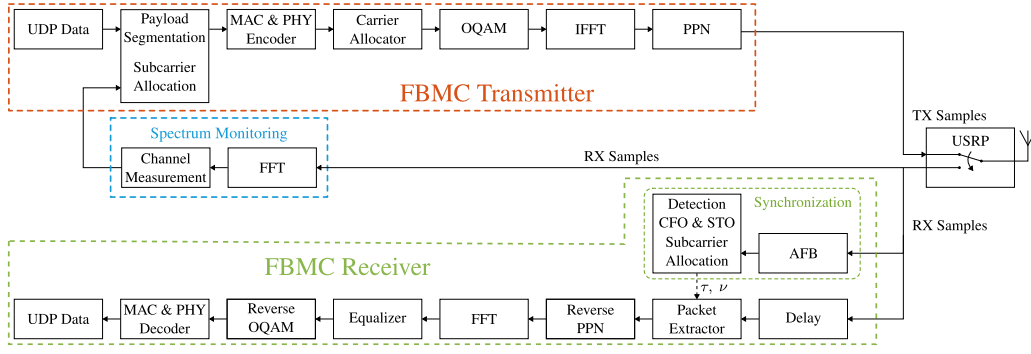


Figure 2: Transceiver block diagram.

system is transmitting at these subcarriers and accordingly the transmitter selects a subcarrier allocation that leaves a gap at this part of the spectrum.

B. Receiver

The structure of the receiver starts with the block *USRP* (Figure 2) in receive mode, through which a continuous stream of IQ samples is received. The received FBMC signal $r[nT_s]$ is

$$r[nT_s] = (h[nT_s] * s[nT_s - \tau]) e^{j\frac{2\pi}{T}\nu nT_s} e^{j\Phi} + \eta[nT_s], \quad (2)$$

with channel impulse response $h[nT_s]$, Symbol Timing Offset (STO) τ , Carrier Frequency Offset (CFO) ν , random phase Φ , and additive white Gaussian noise $\eta[nT_s]$.

In the first step, the receiver must detect any FBMC packets and determine which subcarrier allocation the sender picked, as we assume it is unknown to the receiver. For packet detection, samples are first passed through the block *AFB*, which stands for Analysis Filter Bank (AFB). Internally, the AFB reverses the *OQAM*, *IFFT*, and *PPN* operations at the transmitter so that the signal after the AFB in frequency domain yields

$$\tilde{d}_{k,m} = \sum_{n=-\infty}^{\infty} r[nT_s] j^{-(m+k)} p[nT_s - mT/2] e^{-j\frac{2\pi}{T}knT_s}. \quad (3)$$

Given that the preamble consists of two consecutive, identical symbols, we can now correlate the values in Equation (3), and the resulting normalized metric

$$C[m] = \frac{2 \left| \sum_{k \in K_u} \tilde{d}_{k,m} \tilde{d}_{k,m+2}^* \right|}{\sum_{k \in K_u} (|\tilde{d}_{k,m}|^2 + |\tilde{d}_{k,m+2}|^2)} \quad (4)$$

will reach high values once an FBMC packet and its preamble are received. The metric in Equation (4) is blindly computed for each possible subcarrier allocation. Once the metric for one of the allocations exceeds a predefined threshold, we assume a possible packet detection. Furthermore, we ensure that there is a minimum time interval between two packets detections in order to minimize false positive detections. With the presumed position of a FBMC packet and its preamble being known, we can use the preamble to compute estimates for the CFO and STO. The detailed analysis of the estimators is beyond the scope of this work, instead we give all details in [3].

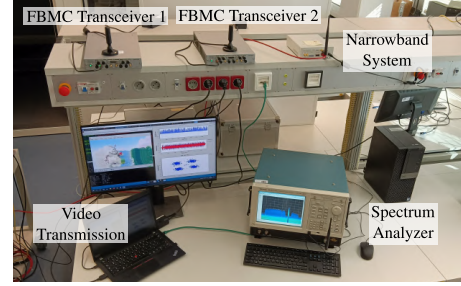


Figure 3: Our testbed setup in a lab environment.

A delayed version of the IQ samples and the estimate for τ and ν are passed into the *Packet Extractor*. This block corrects the CFO and STO and passes packets to the *Reverse PPN* block, which convolves the subcarriers with a matched filter of the prototype filter. After the transformation into frequency domain in the *FFT*, the *Equalizer* follows. The channel is estimated using zero forcing at the pilot tones, and linear interpolation is applied for the remaining subcarriers. The block *Reverse OQAM* follows, in which the factor j^{m+k} is removed and real and imaginary parts are combined back to complex values. Finally, the *MAC & PHY Decoder* follows, in which data is decoded and integrity is ensured via a checksum. The successfully decoded data is passed to the *UDP Data* block, which forwards it to applications such as video players.

III. MEASUREMENTS AND TESTBED DEMONSTRATION

The testbed used for our measurements is shown in Figure 3. It consists of two FBMC transceivers, each using an USRP N310 connected to a computer. In addition, we use a third USRP N210 representing a narrowband system. To observe and record the spectrum, we use a Tektronix RSA6114A spectrum analyzer. In parallel, we measure various parameters of the FBMC transmission such as synchronization metric, constellation diagram, Packet Error Rates (PERs) etc.

The first measurement in Figure 4 demonstrates the steep roll-off possible with the proper FBMC prototype filters. Displayed is the normalized power spectral density versus frequency at subcarrier index 43 for the subcarrier allocation 3 according to Figure 1. For the measurement, we connect the spectrum analyzer and one of the FBMC transceivers with a cable to fully utilize the dynamic range of the spectrum analyzer. We test two FBMC prototype filters that are popular

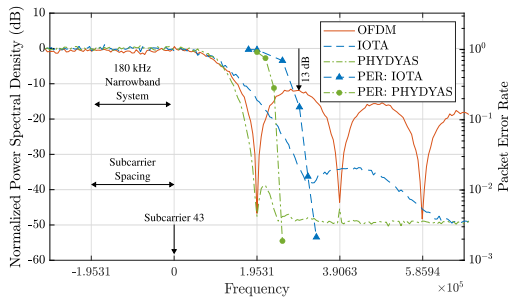


Figure 4: Steepness of roll-off for IOTA and PHYDYAS prototype filter.

in FBMC literature, the Isotropic Orthogonal Transform Algorithm (IOTA) filter [5] and PHYDYAS based on extended gaussian functions [6]. Furthermore, for reference, we show the roll-off of an OFDM rectangular filter that has approximately 13 dB attenuation at the first side lobe.

The roll-off of the IOTA is initially flatter in comparison to the rectangular filter, however, the stop-band attenuation is much better. For the PHYDYAS filter, the attenuation of approximately 48 dB at the frequency of the first OFDM side lobe is significantly larger compared to the rectangular filter. It is noted that the theoretical stop-band attenuation of the PHYDYAS filter is even larger at about 60 dB, however, the hardware inaccuracies of the USRPs such as non-linearities and the finite word length when generating the FBMC signal are also reflected by the measurement, which is why the noise floor is higher. Nevertheless, the FBMC prototype filters exhibit better selectivity than OFDM and, thus, they produce less interference at adjacent frequencies and are less susceptible to interference from adjacent systems.

In the second measurement, we demonstrate the coexistence capability of FBMC by means of an application: One of the FBMC transceivers transmits a video file at a data rate of approximately 3.8 Mbit/s, which is received, decoded, and played by the second transceiver. The packet rate averages 1070 frames per second, so each packet contains an average of 440 bytes. We transmit in our lab at a carrier frequency of 755 MHz with a nominal bandwidth of 12.5 MHz. A second narrowband system continuously transmits in parallel, the generated signal is white noise with 180 kHz bandwidth. The carrier frequency of the narrowband system is variable and it can change frequency abruptly. We assume that the narrowband system has less total transmit power than a single FBMC transceiver, but due to the lower bandwidth it has a higher power spectral density. The goal is to show that despite the narrowband system continuously changing its center frequency, the FBMC system is able to autonomously adapt and put a gap around the narrowband carrier. Whether the FBMC system is affected by the narrowband system can be observed, on the one hand, by errors in the video transmission and, on the other hand, by an increasing PER. If the FBMC system were non-adaptive and the narrowband 180 kHz system were moved close to the occupied FBMC subcarriers, PERs would result as shown in Figure 4 on the right axis. For the PHYDYAS filter, a spacing of 1.25 subcarriers is sufficient to achieve a PER of less than $1e-2$.

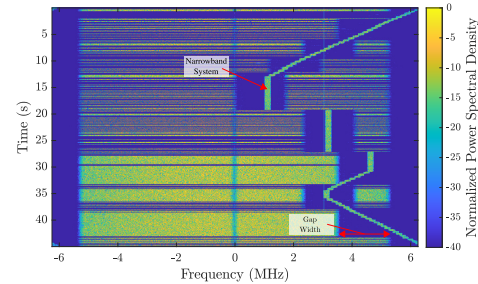


Figure 5: Spectrogram of our FBMC system and a moving narrowband system.

In Figure 5 a spectrogram diagram of the video transmission is shown, recorded over a duration of 45 seconds and a bandwidth of 12.5 MHz. The horizontal yellow lines represent FBMC packets whose density depends on the instantaneous data rate of the video encoder. The narrowband system moves across the right side of the spectrum and the FBMC system adjusts accordingly. Since the measurement was performed in our laboratory with optimal channel conditions (line of sight, flat channel, small distances), we measure no change of the packet error rate of the FBMC transmission with or without the narrowband system. In the future, we will move our measurements to more complex channel environments where we expect performance degradation, e.g., due to fading of the narrowband signal.

IV. CONCLUSION

In this work, we have presented an open-source wireless multicarrier system that combines three special features: it uses FBMC as a modulation scheme, it synchronizes received signals in frequency domain, and it can autonomously adjust its own bandwidth to coexisting systems in the same frequency range. We have given an overview of the structure of the FBMC transceiver and by performing measurements showed that for the implemented bandwidth adaptation, FBMC is more suitable than OFDM. As the complete project is freely available online, it can be tested and extended by other researchers as desired.

REFERENCES

- [1] S. Hu, Q. Luo, J. Zhang, D. Huang, Z. Liu, and Y. Gao, "Practical Implementation of MIMO-FBMC System," in *Communications, Signal Processing, and Systems*, Q. Liang, X. Liu, Z. Na, W. Wang, J. Mu, and B. Zhang, Eds. Singapore: Springer Singapore, 2019, pp. 10–18.
- [2] F. Wunsch, S. Koslowski, S. Müller, N. Cuervo, and F. K. Jondral, "A cognitive overlay system based on fbmc," in *2017 IEEE International Symposium on Dynamic Spectrum Access Networks (DySPAN)*, 2017.
- [3] C. Thein, M. Schellmann, and J. Peissig, "Analysis of frequency domain frame detection and synchronization in OQAM-OFDM systems," *EURASIP Journal on Advances in Signal Processing*, vol. 2014, 11 2014.
- [4] M. Penner, S. Akin, M. Fuhrwerk, and J. Peissig, "Bit Error Probability for Asynchronous Channel Access with Interference Cancellation and FBMC," in *2020 IEEE Wireless Communications and Networking Conference (WCNC)*, 2020.
- [5] P. Siohan and C. Roche, "Cosine-modulated filterbanks based on extended Gaussian functions," *IEEE Transactions on Signal Processing*, vol. 48, no. 11, pp. 3052–3061, 2000.
- [6] M. Bellanger, "Specification and design of a prototype filter for filter bank based multicarrier transmission," in *2001 IEEE International Conference on Acoustics, Speech, and Signal Processing. Proceedings (Cat. No.01CH37221)*, vol. 4, 2001, pp. 2417–2420 vol.4.